

# VLA and VLBA Observations of the Highest Redshift Radio-Loud QSO J1427+3312 at $z = 6.12$

Emmanuel Momjian<sup>1</sup>

*NAIC, Arecibo Observatory, HC 3, Box 53995, Arecibo, PR 00612*

emomjian@naic.edu

Christopher L. Carilli

*National Radio Astronomy Observatory, P. O. Box O, Socorro, NM, 87801*

ccarilli@nrao.edu

Ian D. McGreer

*Department of Astronomy, Columbia University, 550 West 120th Street, New York, NY  
10027*

mcgreer@astro.columbia.edu

## ABSTRACT

We present 8.4 GHz VLA A-array and 1.4 GHz VLBA results on the radio continuum emission from the highest redshift radio-loud quasar known to date, the  $z = 6.12$  QSO J1427+3312. The VLA observations show an unresolved steep spectrum source with a flux density of  $250 \pm 20 \mu\text{Jy}$  at 8.4 GHz and a spectral index value of  $\alpha_{1.4}^{8.4} = -1.1$ . The 1.4 GHz VLBA images reveal several continuum components with a total flux density of  $1.778 \pm 0.109 \text{ mJy}$ , which is consistent with the flux density measured with the VLA at 1.4 GHz. Each of these components is resolved with sizes of a few milliarcseconds, and intrinsic brightness temperatures on the order of  $10^7$  to  $10^8$  K. The physical characteristics as revealed in these observations suggest that this QSO may be a Compact Symmetric Object, with the two dominant components seen with the VLBA, which are separated by 31 mas (174 pc) and have intrinsic sizes of  $\sim 22\text{--}34 \text{ pc}$ , being the two radio lobes that are confined by the dense ISM. If indeed a CSO, then the estimated kinematic age of this radio AGN is only  $10^3$  yr.

*Subject headings:* galaxies: individual (J1427+3312) — galaxies: active — galaxies: high-redshift — radio continuum: galaxies — techniques: interferometric

---

<sup>1</sup>now at: National Radio Astronomy Observatory, P. O. Box O, Socorro, NM, 87801, emomjian@nrao.edu

## 1. INTRODUCTION

Optical surveys such as the Sloan Digital Sky Survey (SDSS; York et al. (2000)) and the Digitized Palomar Sky Survey (Djorgovski et al. 1999) have revealed large samples of quasi-stellar objects out to  $z \sim 6$ . Studies by Fan et al. (2002, 2006) have shown that at such a high redshift we are approaching the epoch of reionization, the edge of the “dark ages”, when the first stars and massive black holes were formed. Eddington limit arguments suggests that the supermassive black holes at the center of these QSOs are on the order of  $10^9 M_{\odot}$ . If the correlation between bulge and black hole masses (Gebhardt et al. 2000; Ferrarese & Merritt 2000; Kurk et al. 2007) also holds at these high redshifts, then these sources have associated spheroids with masses on the order of  $\sim 10^{12} M_{\odot}$ . It is challenging to explain the formation of such massive structures in relatively short timescales ( $< 1$  Gyr; e.g. Li et al. (2007)). Wyithe & Loeb (2002) estimate that almost one third of known quasars at  $z \sim 6$  ought to be lensed by galaxies along the line of sight. If these quasars are indeed gravitationally lensed, the estimated masses of their associated spheroids could be smaller by up to an order of magnitude; this would allow a less efficient assembly process. However, Kurk et al. (2007) derived black hole masses in a sample of  $z \sim 6$  quasars using the widths of the Mg II and C IV lines. The resulting mass values were comparable and in agreement with those derived by assuming that the quasars emit at their Eddington luminosity, implying that the quasars are not likely to be strongly lensed (Kurk et al. 2007).

High resolution radio observations of high-redshift radio-loud quasars can be used to test for strong gravitational lensing by looking for multiple imaging on scales from tens of milliarcseconds (mas) to arcseconds. Also, Very Long Baseline Interferometry (VLBI) observations of core-jet radio sources in quasars over a large range in redshift have been used to constrain the cosmic geometry, under the assumption that such sources are (roughly) ‘standard rulers’ (Gurvits, Kellermann, & Frey 1999). In general, the high resolution of the VLBI observations permit a more detailed look at the physical structures in the most distant cosmic sources on scales unreachable with any other technique (mas).

To date, several radio-quiet and radio-loud quasars with redshifts  $z > 4$  have been imaged using VLBI (Frey et al. 1997, 2003; Momjian et al. 2004, 2005, 2007). Of these, only two were radio-loud quasars at redshifts  $z > 5$ , namely J0913+5919 at  $z = 5.11$  (Momjian et al. 2004), and J0836+0054 at  $z = 5.82$  (Frey et al. 2003). Furthermore, and until recently, all known  $z > 6$  QSOs were radio-quiet. However, McGreer et al. (2006) reported the discovery of the first radio-loud QSO at a redshift greater than 6, namely the QSO J1427+3312 at  $z = 6.12$ , by matching VLA’s FIRST survey (Becker, White, & Helfand 1995) with the NOAO Deep Wide Field Survey (NDWFS; Jannuzi & Dey (1999)) and the FLAMINGOS EXtragalactic Survey (FLAMEX; Elston et al. (2006)).

In this paper we present 8.4 GHz Very Large Array (VLA) and 1.4 GHz Very Long Baseline Array (VLBA) observations of the highest redshift radio-loud quasar known to date, J1427+3312 at  $z = 6.12$ . At the redshift of the source, observing frequencies of 1.4 and 8.4 GHz correspond to rest frequencies of 10 and 60 GHz, respectively.

The source J1427+3312 is classified as a Broad Absorption Line Quasar (BALQSO; McGreer et al. (2006)), and has a radio flux density of 1.73 mJy at 1.4 GHz (Becker, White, & Helfand 1995). This QSO is not detected in the *Chandra* XBoötes survey (Murray et al. 2005), implying an upper limit in the 0.5-7 KeV band of  $4 \times 10^{-15}$  erg cm<sup>-1</sup> s<sup>-1</sup>.

Spectra obtained with the Keck II telescope reveal two strong Mg II absorption systems, one at  $z = 2.1804$  and another at  $z = 2.1997$  (McGreer et al. 2006). The presence of these absorption systems in the line-of-sight raises the possibility that the QSO is being gravitationally lensed.

Throughout this paper, we assume a flat cosmological model with  $\Omega_m = 0.3$ ,  $\Omega_\Lambda = 0.7$ , and  $H_0 = 71$  km s<sup>-1</sup> Mpc<sup>-1</sup>. In this model, at the distance of J1427+3312, 1 mas corresponds to 5.6 pc.

## 2. OBSERVATIONS AND DATA REDUCTION

### 2.1. VLA Observations

The QSO J1427+3312 was observed with the Very Large Array (VLA) of the NRAO<sup>1</sup> in A configuration on 2007 July 9. The frequency of the observations was 8.4 GHz and the total bandwidth was 100 MHz in both right and left-hand circular polarizations. The source 3C286 was used as the primary flux calibrator, and J1416+3444 as the phase calibrator. The total time was 6 hours with 23 antennas participating in the observations. The VLA data was reduced using standard Astronomical Image Processing System (AIPS) routines. Table 1 summarizes the parameters of the VLA observations.

### 2.2. VLBA Observations

The VLBI observations of J1427+3312 were carried out at 1.4 GHz on 2007 June 11 and 12, using the Very Long Baseline Array (VLBA) of the NRAO. Eight adjacent 8 MHz

---

<sup>1</sup>The National Radio Astronomy Observatory is a facility of the National Science Foundation operated under cooperative agreement by Associated Universities, Inc.

baseband channel pairs were used in the observations, both with right and left-hand circular polarizations, and sampled at two bits. The data were correlated at the VLBA correlator in Socorro, NM, with 2 s correlator integration time. The total observing time was 12 hr. Table 2 summarizes the parameters of the VLBA observations.

The VLBA observations employed nodding-style phase referencing, using the calibrator J1422+3223 ( $S_{1.4 \text{ GHz}} = 0.4 \text{ Jy}$ ), with a cycle time of 4 min, 3 min on the target source and 1 min on the calibrator. The angular separation between the target source and the phase calibrator is  $1.4^\circ$ . A number of test cycles were also included to monitor the coherence of the phase referencing. These tests involved switching between two calibrators, the phase calibrator J1422+3223 and the phase-check calibrator J1416+3444 ( $S_{1.4 \text{ GHz}} = 1.9 \text{ Jy}$ ), using a similar cycle time to that used for the target source. The angular separation between the phase calibrator and the phase-check calibrator is  $2.7^\circ$ .

The accuracy of the phase calibrator position is important in phase-referencing observations (Walker 1999), as this determines the accuracy of the absolute position of the target source and any associated components. Phase referencing, as used here, is known to preserve absolute astrometric positions to better than  $\pm 0''.01$  (Fomalont 1999).

Data reduction and analysis were performed using AIPS of the NRAO. After applying *a priori* flagging, amplitude calibration was performed using measurements of the antenna gain and system temperature for each station. Ionospheric corrections were applied using the AIPS task “TECOR”. The phase calibrator J1422+3223 was self-calibrated in both phase and amplitude and imaged in an iterative cycle.

Images of the phase-check calibrator, J1416+3444, were deconvolved using two different approaches: (a) by applying the phase and the amplitude self-calibration solutions of the phase reference source J1422+3223 (Figure 1a), and (b) by self calibrating J1416+3444 itself, in both phase and amplitude (Figure 1b). The peak surface brightness ratio of the final images from the two approaches gives a measure of the effect of residual phase errors after phase referencing, i.e., ‘the coherence’ due to phase referencing (Moran & Dhawan 1995). At all times, the coherence was found to be better than 99%.

The self-calibration solutions of the phase calibrator, J1422+3223 (Fig. 2), were applied on the target source, J1427+3312, which was then deconvolved and imaged.

### 3. RESULTS & ANALYSIS

Figure 3 is a uniformly weighted image of the  $z = 6.12$  QSO J1427+3312 obtained with the VLA A-array at 8.4 GHz and  $0''.19$  (1.1 kpc) resolution. The detected radio source is unresolved and the measured total flux density is  $250 \pm 20 \mu\text{Jy}$ . No other continuum features were found on scales of several arcseconds.

Comparing the 8.4 GHz flux density with previous 1.4 GHz measurements (Becker, White, & Helfand 1995; Ciliegi et al. 1999) shows that this QSO is a steep spectrum source with a spectral index of  $\alpha_{1.4}^{8.4} = -1.1$ .

Figure 4 is a naturally weighted image of the target source at the full resolution of the VLBA, which is  $11.6 \times 7.8 \text{ mas}$  ( $65 \times 42 \text{ pc}$ ,  $\text{PA}=2^\circ$ ). The rms noise level in this image is  $28 \mu\text{Jy beam}^{-1}$ .

Table 3 lists the Gaussian fitting parameters of the compact continuum sources seen in the VLBA image (Fig. 4) derived using the AIPS task JMFIT. Gaussian components provide a convenient parameterization of source structure even if they do not necessarily represent discrete physical structures. Columns (2) and (3) are the coordinates of the sources, and column (4) is the relative positions of the these sources with respect to the strongest component. Column (5) lists the surface brightnesses of these sources, and column (6) their integrated flux densities. Column (7) gives the nominal deconvolved sizes of the Gaussian components at FWHM as given by JMFIT, and column 8 lists the position angles of the fitted Gaussians. The corresponding intrinsic brightness temperatures of these compact sources are on the order of  $10^7$  to  $10^8 \text{ K}$ , and are listed in column 9.

Based on the VLBA results, the source is composed of two dominant structures separated by  $\sim 31 \text{ mas}$ . The stronger of these is consistent with two Gaussians (components 1 and 3 in Table 3), while the second dominant source is represented by one Gaussian (component 2 in Table 3). Including a possible faint component to the east (component 4 in Table 3), gives a total flux density of  $1.778 \pm 0.109 \text{ mJy}$ . This value is consistent with the  $1.73 \pm 0.13 \text{ mJy}$  obtained with the VLA FIRST survey (Becker, White, & Helfand 1995), and with the  $1.816 \pm 0.021 \text{ mJy}$  obtained with the VLA ELAIS survey (Ciliegi et al. 1999). The 1.4 GHz flux densities measured with the VLA in 1995 and 1997 (Becker, White, & Helfand 1995; Ciliegi et al. 1999) and the VLBA in 2007 (this paper) are equal to better than 5%, implying that this source is not highly variable on time scales of years.

We have also synthesized larger images ( $2'' \times 2''$ ) using the VLBA and found no other radio components at  $\geq 5\sigma$  level ( $140 \mu\text{Jy beam}^{-1}$ ) in the field other than those seen in Figure 4 and listed in Table 3.

#### 4. DISCUSSION

We have detected the  $z = 6.12$  QSO J1427+3312 at 8.4 GHz with the VLA A-array and at 1.4 GHz with the VLBA. The source is unresolved as seen in the 8.4 GHz VLA results, and has a steep spectrum with a spectral index value of  $\alpha_{1.4}^{8.4} = -1.1$ .

At mas resolution, the VLBA observations show that this QSO is comprised of two dominant continuum components separated by 31 mas (174 pc; Table 3) with a flux density ratio of  $\sim 3 : 1$ . The Gaussian fitting suggests that both components are resolved with sizes of  $\sim 4 - 6$  mas (22 – 34 pc).

The physical properties observed in this source suggest that this high- $z$  QSO could be a Compact Symmetric Object (CSO) with two distinct, steep spectra, radio lobes that are confined by a dense ISM in the host galaxy (Conway 2002). CSOs are radio sources that have sizes on scales of 1 pc to 1 kpc, and are thought to be very young ( $\leq 10^4$  yr; Readhead et al. (1996); Owsianik & Conway (1998)). Moreover, because CSOs are highly confined sources, they are thought to have higher conversion efficiency of jet kinetic energy to radio luminosity.

For J1427+3312, the radio lobes would be the two dominant components seen in the 1.4 GHz VLBA results, which are separated by 174 pc. In this model, the core, which would have an inverted or flat spectrum (Taylor, Readhead, & Pearson 1996), would be faint and below our detection threshold. In CSOs, any radio component that is coincident with the central engine is comparatively weak, with flux densities of only a few percent of the total flux density (Readhead et al. 1996).

Classifying this source as a CSO, where the radio lobes are confined by a dense ambient medium, is also consistent with its being a BALQSO (McGreer et al. 2006). This is in agreement with recent X-ray observations which suggest that the presence of massive, highly ionized, and high-velocity outflows in BALQSOs may be providing significant feedback to the surrounding gas (Chartas et al. 2007). In general, the higher average gas densities expected in the earliest galaxies might lead to a higher fraction of CSO sources.

Multi-epoch and multi-frequency VLBI observations carried out by Taylor et al. (2000) on three CSOs have shown typical advance speeds of  $\sim 0.3c$ . Adopting this value for J1427+3312, and assuming equal speeds for the two radio lobes, we derive a kinematic age of  $\sim 10^3$  yr, indicating that the  $z = 6.12$  QSO is a very young radio source.

With overwhelming majority of CSOs ( $\geq 80\%$ ) showing HI 21 cm absorption lines with optical depth levels between 4% and 40% and line widths ranging between about 50 and 500 km s<sup>-1</sup> (Peck et al. 2000), the  $z = 6.12$  QSO J1427+3312, which is believed to be near the Epoch of Reionization, would be an excellent candidate for HI absorption experiments

to detect the neutral IGM in its host galaxy (Furlanetto & Loeb 2002). Such a search is currently underway using the Giant Meterwave Radio Telescope (GMRT). Knowledge of source structure, as presented herein, is critical for both identifying potential candidates for HI 21 cm absorption searches and for subsequent interpretation of the results.

The high resolution radio imaging presented here sets constraints on the hypothesis that J1427+3312 has undergone strong gravitational lensing resulting in multiple images. The VLA 8.4 GHz imaging rules out multiple images separated by  $> 0''.2$  and with a flux ratio  $< 8 : 1$ . The VLBA 1.4 GHz imaging sets similar constraints down to the mas scale. The expected lensing system for a  $z \sim 6$  quasar is a singular isothermal ellipsoid (SIE), with image pairs having separations  $\lesssim 1''$  and flux ratios  $< 10 : 1$  (Turner et al. 1984). The typical lens system is thus ruled out, and only a high magnification or small separation lensing event is allowed by the images obtained from these radio observations.

On the other hand, the possible faint component in the VLBA image to the east (component 4) has a separation of  $\sim 0''.1$  from the strongest component and a flux ratio of  $\sim 7 : 1$ . While it is highly unlikely that an SIE lens would result in such a small image separation, lensing by a spiral galaxy might. However, spirals are expected to contribute only 10%–20% of gravitational lenses (Turner et al. 1984; Keeton & Kochanek 1998), and  $< 5\%$  of spiral lenses would produce image separations  $\sim 0''.1$  (Bartelmann & Loeb 1998). Thus the a priori likelihood that components 4 and 1 represent a lensed image pair is quite low. Future sensitive VLBI observations at multiple frequencies are needed to measure the spectral energy distribution of the various components seen in the VLBA image and determine whether they have identical physical characteristics.

We also cannot rule out that the continuum features seen in this QSO are core-jet structures. The above mentioned sensitive VLBI observations will be able to address this possibility as well. Furthermore, multi epoch VLBI observations can lead to determine the proper motion of the components seen in J1427+3312, and provide a more accurate estimate of the advance speeds of the radio lobes and the kinematic age of the source, assuming that this  $z = 6.12$  is indeed a CSO, or the proper motion of the jet with respect to the core, if the continuum VLBA results were of core-jet structures.

## 5. ACKNOWLEDGMENTS

The Arecibo Observatory is part of the National Astronomy and Ionosphere Center, which is operated by Cornell University under a cooperative agreement with the National Science Foundation. C. L. C. acknowledges support from the Max-Planck Society and the

Alexander von Humboldt Foundation through the Max-Planck Forschungspreise 2005.

## REFERENCES

- Bartelmann, M., & Loeb, A. 1998, ApJ, 503, 48
- Becker R. H., White, R. L., & Helfand, D. J. 1995, ApJ, 450, 559
- Chartas, G., Brandt, W. N., Gallagher, S. C., & Proga, D. 2007, ApJ, 133, 1849
- Ciliegi, P., et al. 1999, MNRAS, 302, 222
- Conway, J. 2002, NewA Rev., 46, 263
- Djorgovski, S.G. et al. 1999, in *Wide Field Surveys in Cosmology*, ed. S. Colombi & Y. Mellier, (Paris: Editions Frontiers), 89
- Elston, R. J., et al. 2006, ApJ, 639, 816
- Fan, X., Narayanan, V. K., Strauss, M. A., White, R. L., Becker, R.H., Pendericci, L., & Rix, H.-W. 2002, AJ, 123, 1247
- Fan, X., Carilli, C. L., & Keating, B. 2006, ARA&A, 44, 415
- Ferrarese, L., & Merritt, D. 2000, ApJ, 539, L9
- Fomalont, E. B. 1999, in *Synthesis Imaging in Radio Astronomy II*, ed. G. B. Taylor, C. L. Carilli, & R. A. Perley (San Francisco: ASP), 301
- Frey, S., Gurvits, L. I., Kellermann, K. I., Schilizzi, R. T., & Pauliny-Toth, I. I. K. 1997, A&A, 325, 511
- Frey, S., Mosoni, L., Paragi, Z., & Gurvits, L. I. 2003, MNRAS, 343, L20
- Furlanetto, S., & Loeb, A. 2002, ApJ, 579, 1
- Gebhardt, K., et al. 2000, ApJ, 539, L13
- Gurvits, L. I., Kellermann, K. I., & Frey, S. 1999, A& A, 342, 378
- Jannuzi, B. T., & Dey, A. 1999, in ASP Conf. Ser. 191, *Photometric Redshifts and the Detection of High Redshift Galaxies*, ed. R. Weymann et al. (San Francisco: ASP), 111



- Keeton, C. R., & Kochanek, C. S. 1998, *ApJ*, 495, 157
- Kurk, J. D., et al. 2007, *ApJ*, 669, 32
- Li, Y., et al. 2007, *ApJ*, 665, 187
- McGreer, I. D., Becker, R. H., Helfand, D. J., & White, R. L. 2006, *ApJ*, 652, 157
- Momjian, E., Petric, A. O., & Carilli, C. L. 2004, *AJ*, 127, 587
- Momjian, E., Carilli, C. L., Petric, A. O. 2005, *AJ*, 129, 1809
- Momjian, E., Carilli, C. L., Riechers, D., & Walter, F., 2007, *AJ*, 134, 694.
- Moran J. M., & Dhawan , V. 1995, in *Very Long Baseline Interferometry and the VLBA*, eds. J. A. Zensus, P. J. Diamond, and P.J. Napier (San Francisco: ASP), 161
- Murray, S. S., et al. 2005, *ApJS*, 161, 1
- Owsianik, I., & Conway, J. E. 1998, *A&A*, 337, 69
- Peck, A. B., Taylor, G. B., Fassnacht, C. D., Readhead, A. C. S., & Vermeulen, R. C. 2000, *ApJ*, 534, 104
- Readhead, A. C. S., Taylor, G. B., Xu, W., Pearson, T. J., Wilkinson, P. N., & Polatidis, A. G. 1996, *ApJ*, 460, 612
- Taylor, G. B., Readhead, A. C. S., & Pearson, T. J. 1996, *ApJ*, 463, 95
- Taylor, G. B., Marr, J. M., Pearson, T. J., & Readhead, A. C. S. 2000, *ApJ*, 541, 112
- Turner, E. L., Ostriker, J. P., & Gott, J. R., III 1984, *ApJ*, 284, 1
- Walker, C. R. 1999, in *Synthesis Imaging in Radio Astronomy II*, ed. G.B. Taylor, C. L. Carilli, & R. A. Perley (San Francisco: ASP), 433
- Wyithe, J. S. & Loeb, A. 2002, *Nature*, 417, 923
- York, D. G., et al. 2000, *AJ*, 120, 1579

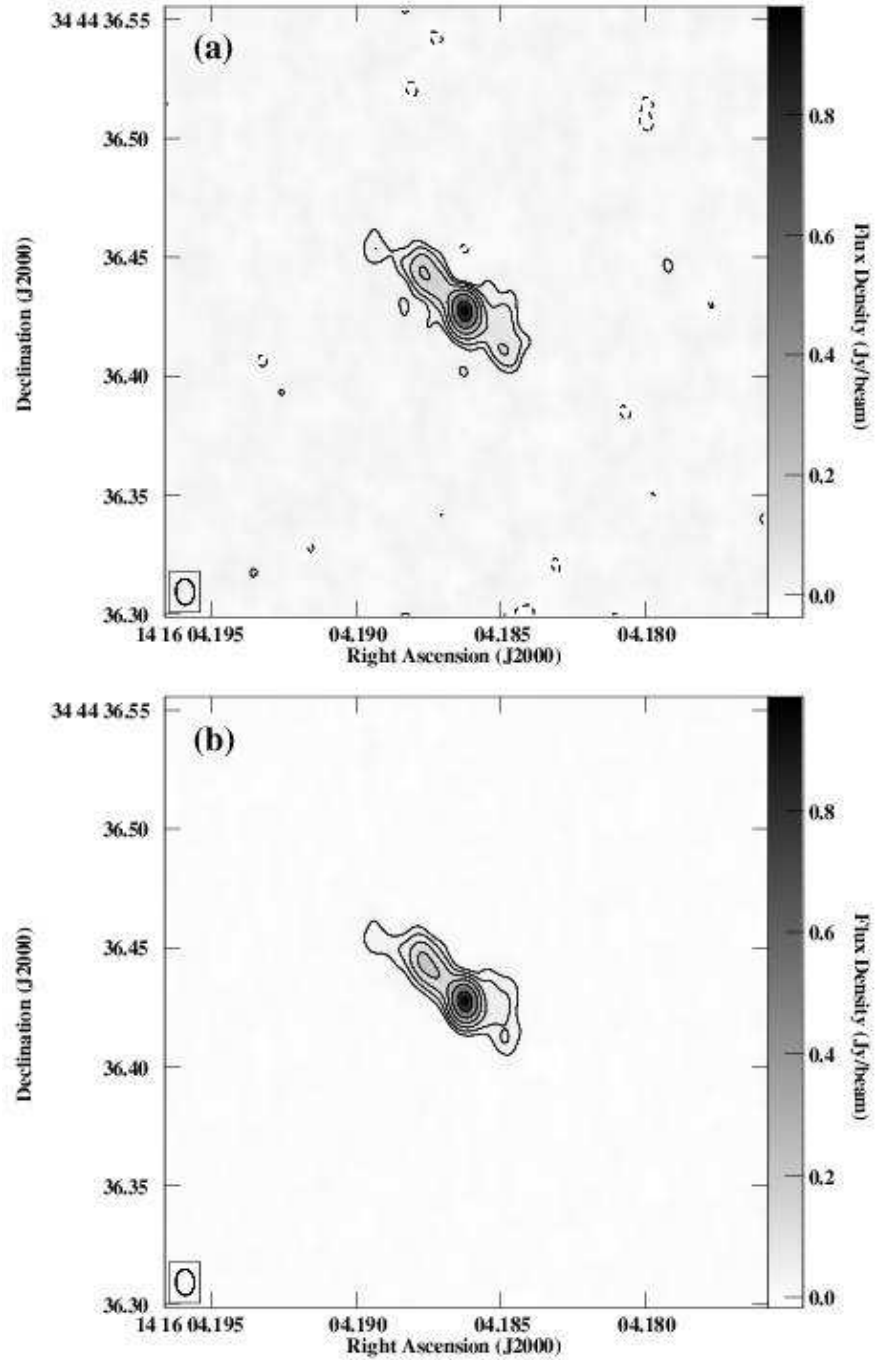


Fig. 1.— VLBA continuum images of the phase-check calibrator J1416+3444 at 1.4 GHz: a) obtained by applying the phase and the amplitude self-calibration solutions of the phase reference source J1422+3223, b) obtained by self-calibrating J1416+3444 itself, in both phase and amplitude. The restoring beam size in both images is  $10.9 \times 7.8$  mas in position angle  $3^\circ$ . The contour levels are at  $-3, 3, 6, 12, \dots, 92$  times the rms noise level in the phase-referenced image (a), which is  $7.1 \text{ mJy beam}^{-1}$ . The gray-scale range is indicated by the step wedge at the right side of each image.

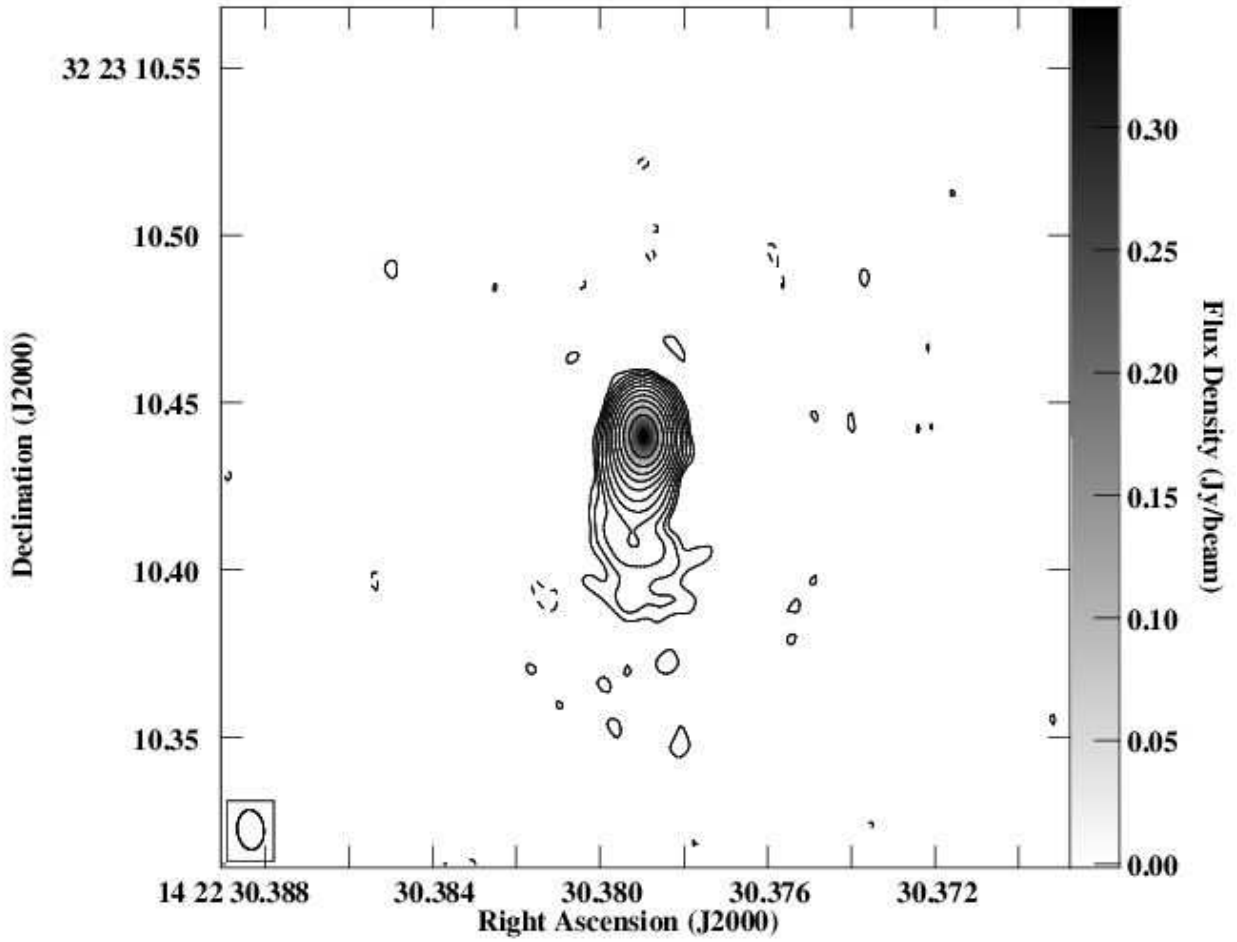


Fig. 2.— VLBA continuum image of the phase calibrator J1422+3223 at 1.4 GHz. The restoring beam size is  $11.9 \times 8.0$  mas in position angle  $5^\circ$ . The contour levels are at  $-3, 3, 6, 12, \dots, 6144$  times the rms noise level, which is  $54 \mu\text{Jy beam}^{-1}$ . The gray-scale range is indicated by the step wedge at the right side of the image.

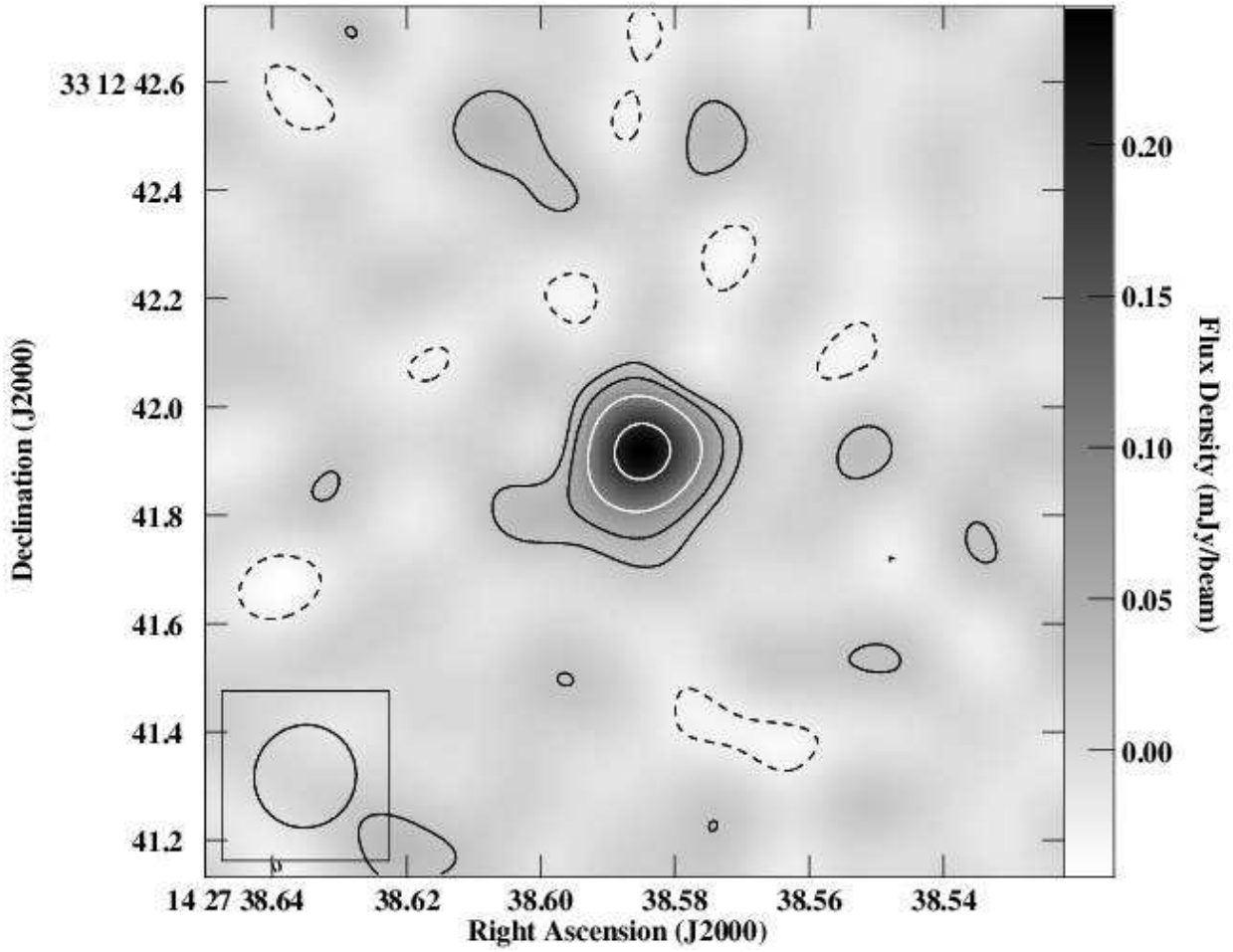


Fig. 3.— Uniformly weighted VLA A-array continuum image of the  $z = 6.12$  QSO J1427+3312 at 8.4 GHz. The restoring beam size is  $192 \times 188$  mas in position angle  $-51^\circ$ . The contour levels are at  $-2, 2, 4, 8, 16$  times the rms noise level, which is  $12.3 \mu\text{Jy beam}^{-1}$ . The gray-scale range is indicated by the step wedge at the right side of the image.

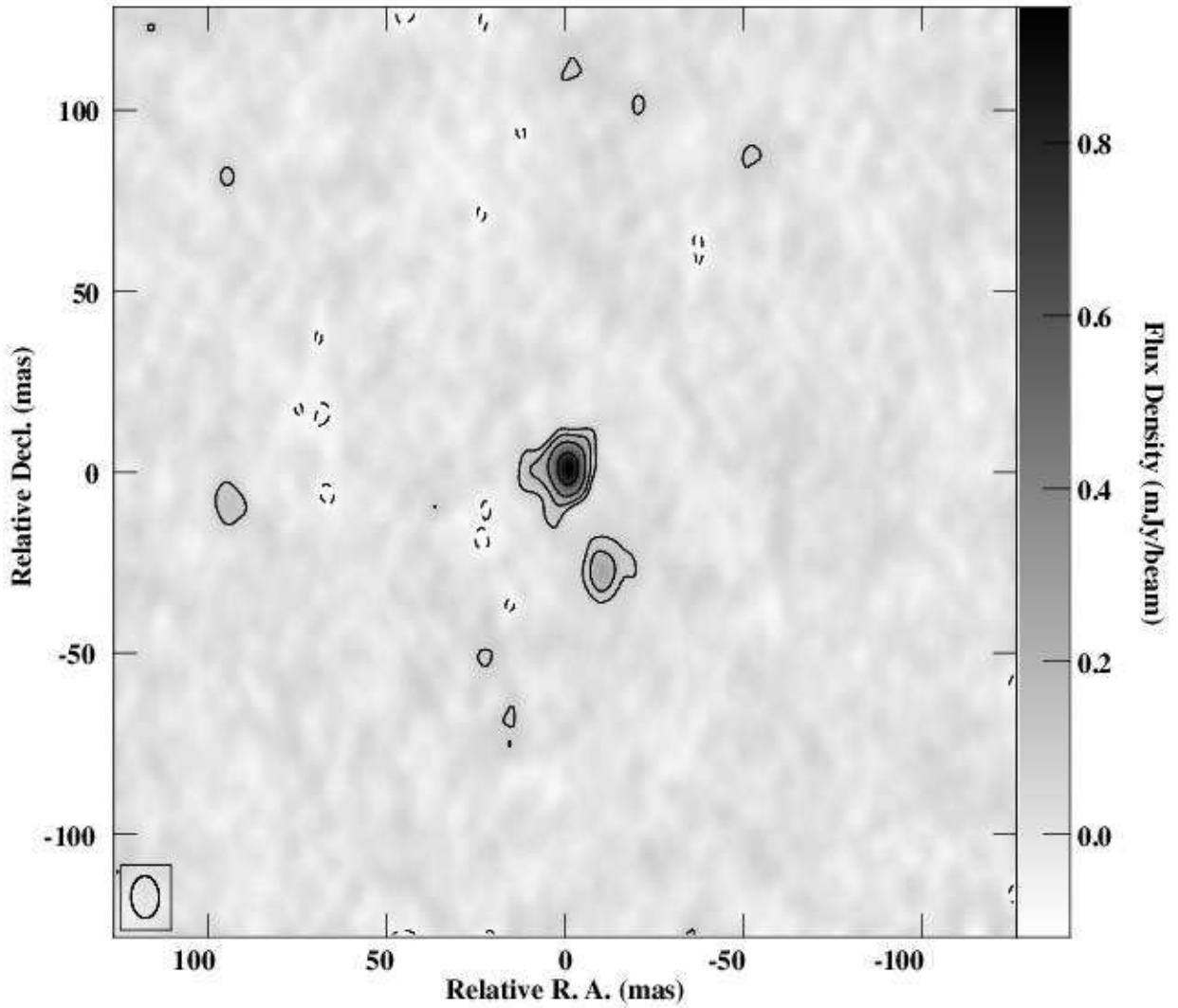


Fig. 4.— Naturally weighted VLBA continuum image of the  $z = 6.12$  QSO J1427+3312 at 1.4 GHz and  $11.6 \times 7.8$  mas resolution (P. A. =  $2^\circ$ ). The peak flux density is  $953 \mu\text{Jy beam}^{-1}$ , and the contour levels are at  $-3, 3, 6, 12, 24$  times the rms noise level, which is  $28 \mu\text{Jy beam}^{-1}$ . The gray-scale range is indicated by the step wedge at the right side of the image. The reference point  $(0, 0)$  is  $\alpha(\text{J2000.0}) = 14^{\text{h}}27^{\text{m}}38^{\text{s}}5858$ ,  $\delta(\text{J2000.0}) = +33^\circ12'41''.927$ .

Table 1. PARAMETERS OF THE VLA OBSERVATIONS OF J1427+3312

Parameters	Values
Observing Date .....	2007 July 9
Total observing time (hr) .....	6
Primary flux calibrator .....	3C286
Phase calibrator .....	J1416+3444
Frequency (GHz) .....	8.4
Total bandwidth (MHz) .....	100
Theoretical noise level ( $\mu\text{Jy beam}^{-1}$ ) ..	9 <sup>a</sup>
Image R.M.S. noise level ( $\mu\text{Jy beam}^{-1}$ )	12

<sup>a</sup>Assumes natural weighting.

Table 2. PARAMETERS OF THE VLBA OBSERVATIONS OF J1427+3312

Parameters	Values
Observing Dates .....	2007 June 11 & 12
Total observing time (hr).....	12
Phase calibrator.....	J1422+3223
Phase-referencing cycle time (min) ....	4
Frequency (GHz).....	1.4
Total bandwidth (MHz).....	64
Theoretical noise level ( $\mu\text{Jy beam}^{-1}$ )..	24 <sup>a</sup>
Image R.M.S. noise level ( $\mu\text{Jy beam}^{-1}$ )	28

<sup>a</sup>Assumes natural weighting.

Table 3. GAUSSIAN FITTING PARAMETERS OF THE CONTINUUM FEATURES IN FIGURE 4

Source	R. A. (J2000)	Decl. (J2000)	Relative Position <sup>a</sup>	Peak <sup>b</sup>	Total	Deconvolved Size <sup>c</sup>	P.A.	$T_b \times 10^7$
(1)	(2)	(3)	(mas)	(mJy beam <sup>-1</sup> )	(mJy)	(mas)	(°)	(K)
(1)	(2)	(3)	(4)	(5)	(6)	(7)	(8)	(9)
1 . . . . .	14 <sup>h</sup> 27 <sup>m</sup> 38 <sup>s</sup> 5857	+33°12'41"928	0, 0	0.958 ± 0.028	1.089 ± 0.053	4.5 × 2.7	173	38.6
2 . . . . .	14 <sup>h</sup> 27 <sup>m</sup> 38 <sup>s</sup> 5850	+33°12'41"899	8.8W, 29S	0.262 ± 0.028	0.343 ± 0.058	7.3 × 3.8	175	5.3
3 . . . . .	14 <sup>h</sup> 27 <sup>m</sup> 38 <sup>s</sup> 5866	+33°12'41"927	11.3E, 1S	0.162 ± 0.028	0.168 ± 0.050	2.2 × 1.5	2	21.9
4 . . . . .	14 <sup>h</sup> 27 <sup>m</sup> 38 <sup>s</sup> 5933	+33°12'41"918	95.4E, 10S	0.143 ± 0.028	0.178 ± 0.056	6.0 × 2.3	56	4.4

<sup>a</sup>With respect to source 1.

<sup>b</sup>Higher than  $5\sigma = 140\mu\text{Jy beam}^{-1}$ .

<sup>c</sup>At half maximum.